

Bright Pulsed Squeezed Light for Quantum-Enhanced Precision Microscopy

Alex Terrasson¹, Lars Madsen¹, Joel Q. Grim², and Warwick. P. Bowen^{1,*}

¹ Australian Research Council Centre of Excellence in Quantum Biotechnology, University of Queensland

² U.S. Naval Research Laboratory. and

* w.bowen@uq.edu.au

Squeezed states of light enable enhanced measurement precision by reducing noise below the standard quantum limit. A key application of squeezed light is nonlinear microscopy, where state-of-the-art performance is limited by photodamage and quantum-limited noise. Such microscopes require bright, pulsed light for optimal operation, yet generating and detecting bright pulsed squeezing at high levels remains challenging. In this work, we present an efficient technique to generate high levels of bright picosecond pulsed squeezed light using a χ^2 optical parametric amplification process in a waveguide. We measure -3.2 dB of bright squeezing with optical power compatible with nonlinear microscopy, as well as -3.6 dB of vacuum squeezing. Corrected for losses, these squeezing levels correspond to $-15.4^{+2.7}_{-8.7}$ dB of squeezing generated in the waveguide. The measured level of bright amplitude pulsed squeezing is to our knowledge the highest reported to date, and will contribute to the broader adoption of quantum-enhanced nonlinear microscopy in biological studies.

I. INTRODUCTION

Stimulated Raman scattering (SRS) imaging is a nonlinear microscopy technique widely used in biological studies for its ability to provide label-free, quantitative, and chemically specific contrast.^{1,2} SRS has been applied to study metabolic processes,³ neuron membrane potentials,⁴ antibiotic responses,⁵ nerve degeneration,⁴ among other biological processes. Improvements in SRS performance would enhance existing studies and enable emerging applications such as high-throughput cancer screening.^{6,7} However photodamage to biological samples limits the usable optical power and therefore the achievable signal level. At the same time, state-of-the-art SRS microscopes are fundamentally limited by the standard quantum limit set by shot noise.^{8,9} As further gains from classical technical improvements diminish, sub-shot noise operation represents the primary pathway toward enhanced SRS sensitivity.¹⁰

Squeezed light is a nonclassical state of light in which a nonlinear interaction redistributes the uncertainty between the two field quadratures, reducing noise in one quadrature below the quantum limit at the expense of increased noise in the other. It was identified as capable of enhancing measurement precision below the standard quantum limit,^{11–13} and high squeezing levels have

been demonstrated for continuous wave and femtosecond pulses.^{14,15} For maximum sensitivity in SRS microscopy, amplitude squeezed light must be generated at high optical power (bright squeezing) and at picosecond (ps) or femtosecond pulse duration, with most systems using ps pulses to match the coherence time of molecular vibrations.¹⁶ In recent years, quantum-enhanced vibrational microscopes have been demonstrated for Brillouin and Raman imaging using bright pulsed squeezed light illumination.^{10,17–21} These works employ either single-mode squeezed light with direct detection or twin-beam intensity-squeezed light with balanced detection, the latter incurring a 3 dB noise penalty compared to direct detection. In both cases, experimental challenges associated with generating and detecting high levels of bright ps pulsed squeezing has limited the level of enhancement achieved.^{16,22}

The highest reported level of ps pulsed squeezing is -5.88 dB,²³ achieved using a single-pass optical parametric amplifier (OPA) based on a periodically poled lithium niobate (PPLN) waveguide. This result relied on advanced temporal and spatial shaping of the local oscillator (LO). Earlier work demonstrated comparable squeezing levels of -5.8 dB using LO-squeezed field co-propagation through the OPA to achieve high spatial overlap;²⁴ however, the corresponding bright squeezing reported in a subsequent study was limited to -0.8 dB.²⁵ In our previous work, we generated and measured -1.8 dB of bright amplitude pulsed squeezing²⁰ using a single-pass OPA based on a PPKTP crystal. In that approach, a bright field was used to seed the OPA and direct detection was performed, with a custom detector that was able to tolerate the high peak intensities. Parasitic multimode effects associated with this configuration limited the measured squeezing level.

In this work, we present a bright, pulsed squeezed-light source capable of high levels of amplitude squeezing at power levels used in state-of-the-art SRS microscopes.^{9,10} We generate the squeezed field in a single pass OPA using a PPLN waveguide. Spatial overlap is achieved by co-propagating the LO with the squeezed field through the waveguide. The field is then displaced by the LO into a bright squeezed field with a set of wave-plates and polarizing beam splitter (PBS). We report -3.2 dB of bright squeezing in direct detection at a displaced optical power of 3.2 mW, and -3.6 dB of squeezing measured via homodyne detection. The observed squeezing level is primarily limited by losses, in particular the quantum efficiency (QE) of the photodetectors at 0.75. After correcting for the losses, those measured squeezing levels correspond to $-15.4^{+2.7}_{-8.7}$ dB

generated within the waveguide. The spatial mode overlap between squeezed field and the LO is simulated to be 99.7%, while the temporal mode overlap is experimentally measured to be 97.7%. This experimental approach opens a pathway towards higher levels of generated and detected bright squeezed light, a key requirement for the broader adoption of quantum-enhanced nonlinear microscopy in biological studies.

II. EXPERIMENTAL SETUP

The experimental setup is shown in Figure 1. A dual-head laser provides synchronized fundamental and second-harmonic beams at 1064 nm and 532 nm with 6 ps pulses and 80 MHz repetition rate. The beams are combined and focused by a microscope objective (PAL-20-NIR-LCOO objective, Optosigma) into a 5-mm-long periodically poled MgO-doped lithium niobate ridge waveguide with AR-coated facets(HC Photonics). The short waveguide length limits the effect of group velocity mismatch between the green pump and the 1064 nm seed. An oven (TC-038D) sets the temperature to the phase-matching temperature.

The polarization of the 1064 nm beam is adjusted such that only a small fraction seeds the OPA process. The 532 nm field pumps the OPA, generating the squeezed vacuum. The rest of the 1064 nm power is polarized along the ordinary axis of the waveguide and serves as the LO. Single-mode confinement in the waveguide ensures high spatial mode matching between the squeezed field and the LO. The output fields are collected with a lens (C330TMD, NA=0.7). The second harmonic beam is separated and used as input in a Pound Drever Hall (PDH) locking scheme^{10,26} to stabilize the relative phase between the OPA pump and seed. A set of waveplates (WP1-3) controls the relative phase between LO and squeezed vacuum and sets the splitting ratio at a polarizing beam splitter (PBS1). In more detail, WP1 converts the two linear polarizations into left- and right-handed circular polarizations. WP2 controls the relative phase between these components, thereby setting the squeezing angle. WP3 converts the field back towards linear polarization, determining the splitting ratio at PBS1.

Adjusting WP2 to amplitude squeezing and WP3 to a 90/10 splitting ratio generates a bright amplitude-squeezed beam with 10% of the LO power (at the cost of a 10% loss on the squeezed field). Separate phase locking of the LO and squeezed field is not required as the LO and seed co-propagate. In this configuration, bright squeezing is measured in direct detection with a custom photodetector compatible with SRS microscopy (see previous work¹⁰ for details). Homodyne detection²⁷ can also be performed when WP3 sets a 50/50 splitting ratio and both output ports are detected, the enables to measure quadrature squeezing in addition to amplitude squeezing. In both configurations, the noise spectrum is recorded using a low-noise spectrum analyzer (N9010A,

Agilent).

In previous work,^{10,20} bright amplitude squeezing was generated by seeding the OPA with a bright field, eliminating the need for a spatially and temporally matched LO and compatible with direct detection. This approach, however, introduces an equivalent mode-matching requirement between the seed and the OPA pump: any seed component not overlapping with the pump is detected at the shot-noise level without deamplification, causing its relative contribution to increase with deamplification. To mitigate this limitation, we adopt a weakly seeded OPA followed by displacement after the OPA using a matched LO. In this configuration, imperfect LO–signal overlap reintroduces shot noise, but its contribution is not amplified, resulting in improved robustness of the squeezing measurement.

We quantify the spatial overlap η_{spatial} between the self-matched LO and the squeezed field using finite-element simulations performed in COMSOL. The spatial overlap in the far field, where interference occurs at PBS1, is identical to the modal overlap in the waveguide. We therefore simulate the guided modes along the ordinary and extraordinary waveguide axes, with refractive indices of 2.2288 and 2.1474, respectively.²⁸ The corresponding 2D spatial mode profiles are shown in Figure 2, a). The optical confinement provided by the waveguide yields a spatial overlap of $\eta_{\text{spatial}} = 0.997$.

In an ideal OPA process, the squeezed field has the same pulse duration as the pump; therefore, we experimentally characterize temporal overlap by measuring the LO and pump pulse durations. This is done using a free space interferometric autocorrelation setup where the interference fringes are scanned with a piezo-mounted mirror, and the visibility is recorded as a function of delay. The results are shown Figure 2, b) where the red and green markers corresponds to the measured visibilities for the 1064 and 532 nm, respectively, and the solid lines are a Gaussian fit to the data. From these fits, we extract pulse durations of $\tau_{\text{LO,exp}} = 6.4 \pm 0.07$ ps and $\tau_{\text{pump,exp}} = 5.17 \pm 0.15$ ps, yielding an experimental temporal overlap of $\eta_{\text{temp,exp}} = 0.977 \pm 0.006$. The measured pump pulse duration is 14% longer than the ideal value, which we attribute to group velocity broadening in the second-harmonic generation stage.

Temporally shaping the LO to match the squeezed field pulse duration can further increase the temporal overlap. This approach has been demonstrated by propagating the LO through a second optical parametric amplifier (OPA).²⁹ In that work, however, imperfect temporal overlap accounted for a significant fraction of the total optical loss. In the present system, the measured temporal overlap results in only 2.3% loss. Moreover, temporal shaping of the LO using an OPA modifies its photon-number statistics. While this does not affect homodyne detection due to common-mode rejection in the balanced measurement, it can degrade squeezing measurements based on direct detection, where the photon statistics of the LO directly contribute to the detected

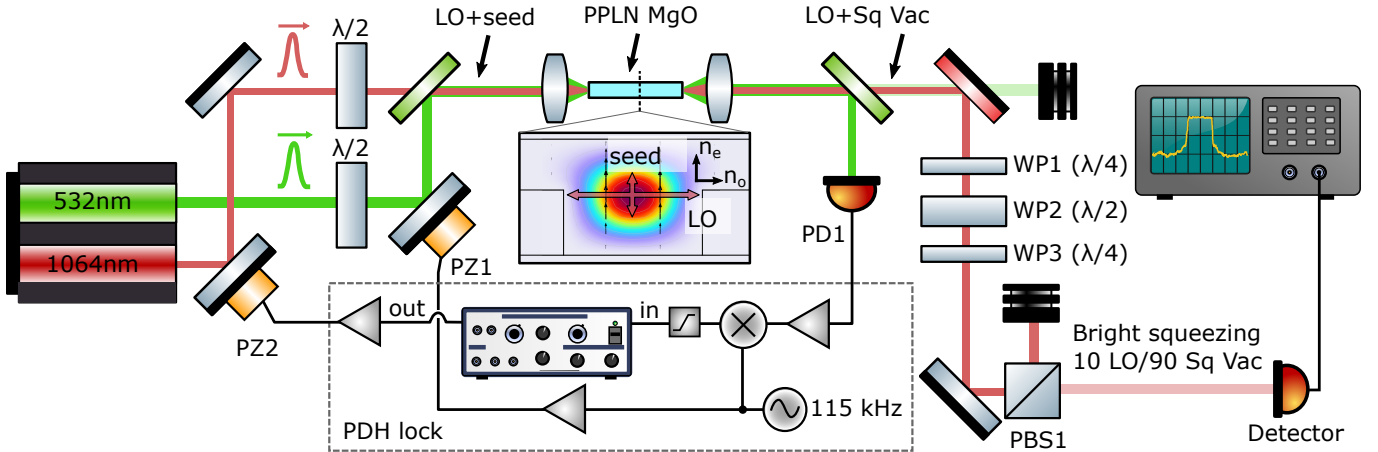


FIG. 1. **Experimental setup** A dual-head laser generates synchronized 1064 nm and 532 nm light pulses with 6 ps and 80 MHz repetition rate. The beams are recombined and focused into a periodically poled MgO-doped lithium niobate (PPLN) waveguide. The 1064 beam is polarized along the ordinary axis of the waveguide and serves as the LO. A weak component polarized along the extraordinary axis seeds the OPA and generates squeezed vacuum. The 532 nm beam is detected and used to lock the relative phase between the 1064 nm and 532 nm fields using a PDH lock scheme. The LO and squeezed vacuum are recombined and mixed at a PBS using three waveplates (WP 1-3). After the PBS, the field is detected either in a balanced homodyne configuration with a 50/50 mixing ratio using two photodetectors (not shown) or with a 90/10 mixing ratio at a single output to generate bright squeezing.

noise.

III. SQUEEZED LIGHT MEASUREMENT

We measure squeezing using both balanced homodyne detection and direct detection. Pulsed quadrature squeezing is characterized using balanced homodyne detection. The homodyne detector is balanced by adjusting WP3 to achieve a 50/50 splitting ratio at PBS1, with 3.2 mW of LO power incident on each photodetector. The vacuum squeezing level is obtained by subtracting the photocurrents from the two detector outputs.

We vary the OPA pump power while monitoring the squeezing and antisqueezing levels at a sideband frequency of 20 MHz. Switching between the squeezed and antisqueezed quadratures is achieved by rotating the half-wave plate WP2. The shot-noise reference is obtained by blocking the OPA pump, thereby suppressing the signal at the PBS1 signal port. Figure 3(a) shows the squeezing and antisqueezing levels as a function of pump power after subtraction of the electronic noise (green and orange markers, respectively). Figure 3(b) shows representative noise spectra of the squeezed, antisqueezed, shot-noise, and electronic-noise signals at a pump power of 20 mW. At this frequency, we observe -3.61 ± 0.05 dB of squeezing and 13.54 ± 0.02 dB of antisqueezing. The electronic-noise clearance is 13.2 dB, corresponding to a squeezing level of -3.9 dB after electronic-noise subtraction.

To quantify the total detection efficiency and assess the impact of phase noise, we fit the measured squeezing and antisqueezing levels using a standard theoret-

ical model that accounts for optical loss and phase-noise-induced leakage of antisqueezing into the squeezed quadrature:

$$V^\pm(P) = \eta \left[e^{\pm 2\alpha\sqrt{P}} \cos^2 \delta + e^{\mp 2\alpha\sqrt{P}} \sin^2 \delta \right] + 1 - \eta + EN \quad (1)$$

where V^- and V^+ denote the variances of the squeezed and antisqueezed quadratures, respectively; η is the total detection efficiency; $\alpha\sqrt{P}$ is the squeezing parameter with P being the OPA pump power; δ represents phase noise; and EN denotes the electronic noise. $e^{\pm 2\alpha\sqrt{P}}$ corresponds to the squeezing and antisqueezing levels generated in the waveguide. The experimental data are fit in dB units (solid green and orange lines in Fig. 3(a)), yielding $\eta_{\text{total,fit}} = 0.61 \pm 0.02$, $\delta = 12 \pm 30$ mrad, and $\alpha = 12.4 \pm 0.1$ mW $^{1/2}$. The large uncertainty in δ reflects the fact that the observed squeezing is primarily limited by optical losses rather than by phase noise.

The total efficiency η_{total} arises from several contributions: waveguide losses η_{wg} (including scattering, green-induced infrared absorption (GRIIRA), photorefractive effects and group velocity mismatch between the seed and pump³⁰⁻³³), propagation losses between the waveguide and the detectors $\eta_{\text{prop}} = 0.96$, spatial and temporal mode overlap between the LO and the squeezed field $\eta_{\text{overlap}} = \eta_{\text{spatial}} \cdot \eta_{\text{temp,exp}} = 0.97$, and detector QE $\eta_{\text{det}} = 0.75$. The overall efficiency is therefore given by $\eta_{\text{total,exp}} = \eta_{\text{wg}} \cdot \eta_{\text{prop}} \cdot \eta_{\text{overlap}} \cdot \eta_{\text{det}}$.

Comparing $\eta_{\text{total,exp}}$ with the fitted value $\eta_{\text{total,fit}}$ yields a waveguide efficiency of $\eta_{\text{wg}} = 0.87$, consistent with the literature on LN waveguides.^{29,32} We estimate the squeezing generated in the waveguide V_{wg}^- by cor-

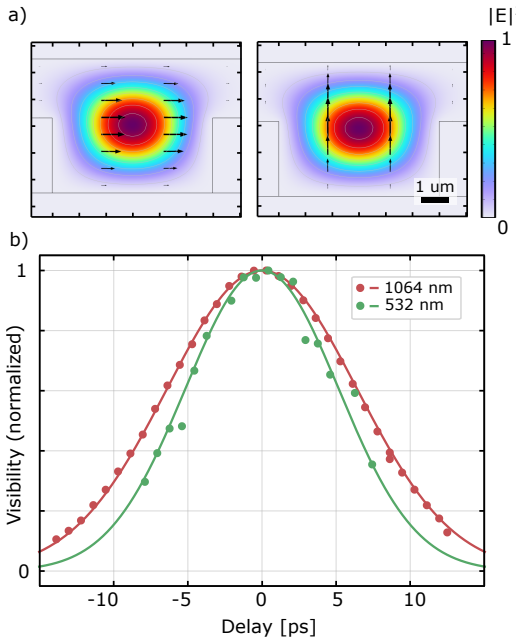


FIG. 2. Spatial and temporal overlap between the LO and squeezed field **a)** COMSOL modal analysis of the waveguide modes for S and P polarizations. The top panel shows the mode intensity for the horizontally polarized mode, corresponding to the LO. The bottom panel shows the mode intensity for the vertically polarized mode, corresponding to the squeezed field. **b)** Experimental measurement of the pulse durations of the LO and OPA pump. Pulse durations are measured using an interferometer by monitoring the interference visibility as the optical path length of one arm is varied. Red markers show the LO data and the solid curve is a Gaussian fit, yielding a pulse duration of $\tau_{\text{LO,exp}} = 6.4 \pm 0.07$ ps. Green markers correspond to the OPA pump, with a fitted pulse duration of $\tau_{\text{pump,exp}} = 5.17 \pm 0.15$ ps.

recting for all losses and propagating the uncertainties in $\eta_{\text{total,fit}}$, V^- and δ in Eq.(1). This yields $V_w^- = -15.4^{+2.7}_{-8.7}$ dB. The large lower uncertainty limit arises from operation near the loss-limited lower bound of the measured squeezing. Practical SRS implementations remain subject to waveguide and displacement losses, limiting the bright squeezing level to -6.2 dB. For other on-chip squeezing applications, where only waveguide losses are considered, the corresponding squeezing level is -8.1 dB.

We also perform direct measurement of the bright squeezing, corresponding to the detection scheme used in nonlinear microscopy where the signal is encoded in the optical intensity. To this end, the LO power is increased to approximately 31 mW after the waveguide, and the splitting ratio at PBS1 is set to 90/10, resulting in 3.2 mW directly measured on the photodetector. The reduced fraction of the squeezed field reaching the detector introduces an additional effective loss factor of $\eta_{\text{direct}} = 0.9$. Figure 3(c) shows the measured squeezing

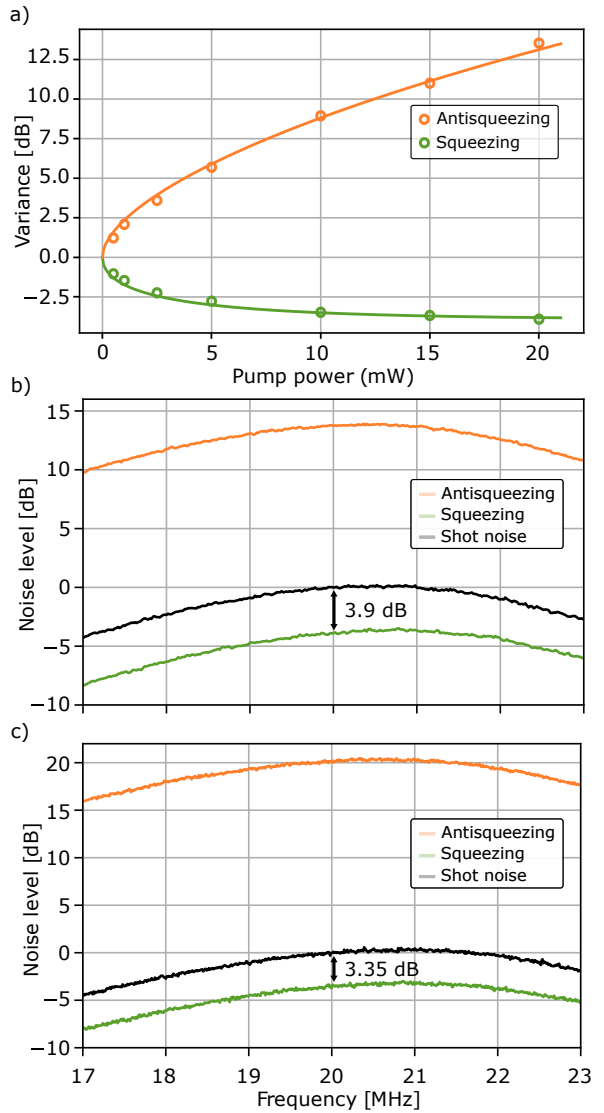


FIG. 3. Squeezed light measurements **a)** Squeezing (green) and antisqueezing (orange) detected in homodyne detection, as a function of pump power. Circles indicate experimental data, solid lines show fits to Eq.(1). **b)** Squeezing (green) and antisqueezing (orange) spectra measured in homodyne detection around 20 MHz for 20 mW of pump power. The black trace is the shotnoise level. A squeezing level of -3.9 dB is obtained after subtracting electronic noise 13.2 dB below shot noise. **c)** Bright squeezing (green) and antisqueezing (orange) spectra with 3.2 mW of coherent amplitude, measured in direct detection. Shot noise is the black trace, the pump power is 40 mW. A squeezing level of -3.35 dB is obtained after subtracting electronic noise 15.3 dB below shot noise.

and antisqueezing levels relative to the shot-noise reference for the bright squeezed beam. A pump power of 40 mW was used, accounting for the larger level of antisqueezing. The measured squeezing level was -3.2 dB, and -3.35 dB after subtracting the electronic noise. This value is consistent with the squeezing measured

previously in homodyne detection: -3.9 dB decreased by an additional 10% of shot noise yields -3.3 dB of observed squeezing.

IV. CONCLUSION

In conclusion, we demonstrate a simple experimental setup that achieves high levels of bright amplitude ps pulsed squeezing. The approach relies on co-propagation of the LO and squeezed field through a single-mode waveguide to achieve high spatial overlap, with waveplates used to control their relative phase and squeezing displacement. We verify spatial and temporal mode overlaps of 99.7% and 97.7%, respectively. We measure -3.35 dB of bright squeezing in a direct-detection configuration at a coherent power of 3.2 mW, compatible with state-of-the-art nonlinear microscopy. After correcting for losses, we infer $-15.4^{+2.7}_{-8.7}$ dB of squeezing generated within the waveguide. The measured squeezing is primarily limited by optical losses, in particular the photodetector QE. High QE photodiodes are available and can be incorporated and after correcting for propagation and detection losses, the expected bright squeezing level for SRS microscopy is -6.2 dB. By achieving this

squeezing level at the photodamage limit of biological samples, an apparatus-independent quantum advantage in microscopy could soon be within reach.

ACKNOWLEDGEMENTS

This research was supported by Defense Advanced Research Projects Agency (DARPA) INSPIRED program (HR00112420356), the Air Force Office of Scientific Research under award numbers FA9550-20-1-0391 and FA9550-22-1-0047, the Australian Research Council Centre of Excellence for Engineered Quantum Systems (EQUS, grant number CE170100009) and the Australian Research Council Centre of Excellence in Quantum Biotechnology (QUBIC, grant number CE230100021). J. Q. Grim was supported by the U.S. Office of Naval Research.

COMPETING INTERESTS

The other authors declare no competing interests.

¹ J.-X. Cheng and X. S. Xie, *Science* **350**, aaa8870 (2015).

² C. H. Camp Jr and M. T. Cicerone, *Nature photonics* (2015).

³ L. Zhang, L. Shi, Y. Shen, Y. Miao, M. Wei, N. Qian, Y. Liu, and W. Min, *Nature biomedical engineering* **3**, 402 (2019).

⁴ F. Tian, W. Yang, D. A. Mordes, J.-Y. Wang, J. S. Salameh, J. Mok, J. Chew, A. Sharma, E. Leno-Duran, S. Suzuki-Uematsu, *et al.*, *Nature communications* **7**, 13283 (2016).

⁵ K. T. Schiessl, F. Hu, J. Jo, S. Z. Nazia, B. Wang, A. Price-Whelan, W. Min, and L. E. Dietrich, *Nature communications* **10**, 762 (2019).

⁶ Q. Cheng, Y. Miao, J. Wild, W. Min, and Y. Yang, *Matter* **4**, 1460 (2021).

⁷ Y. Tan, H. Lin, and J.-X. Cheng, *Science Advances* **9**, eadg6061 (2023).

⁸ B. G. Saar, C. W. Freudiger, J. Reichman, C. M. Stanley, G. R. Holtom, and X. S. Xie, *science* **330**, 1368 (2010).

⁹ C. W. Freudiger, W. Min, B. G. Saar, S. Lu, G. R. Holtom, C. He, J. C. Tsai, J. X. Kang, and X. S. Xie, *Science* **322**, 1857 (2008).

¹⁰ C. A. Casacio, L. S. Madsen, A. Terrasson, M. Waleed, K. Barnscheidt, B. Hage, M. A. Taylor, and W. P. Bowen, *Nature* **594**, 201 (2021).

¹¹ R. Slusher, *Optics and Photonics News* **1**, 27 (1990).

¹² L. Davidovich, *Reviews of Modern Physics* **68**, 127 (1996).

¹³ B. Lawrie, R. Pooser, and P. Maksymovych, *Trends in Chemistry* **2**, 683 (2020).

¹⁴ R. Dong, J. Heersink, J. F. Corney, P. D. Drummond, U. L. Andersen, and G. Leuchs, *Optics letters* **33**, 116 (2008).

¹⁵ H. Vahlbruch, M. Mehmet, K. Danzmann, and R. Schnabel, *Physical review letters* **117**, 110801 (2016).

¹⁶ Z. Xu, S. Nitanai, K. Oguchi, and Y. Ozeki, *Applied Physics Letters* **127** (2025).

¹⁷ Z. Xu, K. Oguchi, Y. Taguchi, S. Takahashi, Y. Sano, T. Mizuguchi, K. Katoh, and Y. Ozeki, *Optics Letters* **47**, 5829 (2022).

¹⁸ T. Li, F. Li, X. Liu, V. V. Yakovlev, and G. S. Agarwal, *Optica* **9**, 959 (2022).

¹⁹ L. Gong, S. Lin, and Z. Huang, *Optics Letters* **48**, 6516 (2023).

²⁰ A. Terrasson, N. P. Mauranyapin, C. A. Casacio, J. Q. Grim, K. Barnscheidt, B. Hage, M. A. Taylor, and W. Bowen, *Optics Express* **32**, 36193 (2024).

²¹ T. Li, V. Cheburkanov, V. V. Yakovlev, G. S. Agarwal, and M. O. Scully, *Proceedings of the National Academy of Sciences* **121**, e2413938121 (2024).

²² X. Heng, L. Zhang, Q. Yin, W. Liu, L. Tang, Y. Zhai, and K. Wei, *Applied Sciences* **15**, 10179 (2025).

²³ J. Amari, J. Takai, and T. Hirano, *Optics Continuum* **2**, 933 (2023).

²⁴ C. Kim and P. Kumar, *Physical review letters* **73**, 1605 (1994).

²⁵ D. Serkland, P. Kumar, M. Arbore, and M. Fejer, *Optics letters* **22**, 1497 (1997).

²⁶ E. D. Black, *American Journal of Physics* (2001).

²⁷ B. L. Schumaker, *Optics letters* **9**, 189 (1984).

²⁸ D. E. Zelmon, D. L. Small, and D. Jundt, *Journal of the Optical Society of America B* **14**, 3319 (1997).

²⁹ Y. Eto, A. Koshio, A. Ohshiro, J. Sakurai, K. Horie, T. Hirano, and M. Sasaki, *Optics letters* **36**, 4653 (2011).

³⁰ M. Bortz, M. Arbore, and M. Fejer, Optics letters **20**, 49 (1995).

³¹ Y. Furukawa, K. Kitamura, A. Alexandrovski, R. Route, M. Fejer, and G. Foulon, Applied Physics Letters **78**, 1970 (2001).

³² M. Bazzan and C. Sada, Applied physics reviews **2** (2015).

³³ M. Jankowski, N. Jornod, C. Langrock, B. Desiatov, A. Marandi, M. Lončar, and M. M. Fejer, Optica **9**, 273 (2022).